



# Passive Online RTT Estimation for Flow-Aware Routers using One-Way Traffic

Damiano Carra, Konstantin Avrachenkov, Sara Alouf, Alberto Blanc, Philippe Nain, Georg Post

## ► To cite this version:

Damiano Carra, Konstantin Avrachenkov, Sara Alouf, Alberto Blanc, Philippe Nain, et al.. Passive Online RTT Estimation for Flow-Aware Routers using One-Way Traffic. [Research Report] RR-7124, INRIA. 2009. inria-00436444v3

**HAL Id: inria-00436444**

**<https://inria.hal.science/inria-00436444v3>**

Submitted on 3 Dec 2009

**HAL** is a multi-disciplinary open access archive for the deposit and dissemination of scientific research documents, whether they are published or not. The documents may come from teaching and research institutions in France or abroad, or from public or private research centers.

L'archive ouverte pluridisciplinaire **HAL**, est destinée au dépôt et à la diffusion de documents scientifiques de niveau recherche, publiés ou non, émanant des établissements d'enseignement et de recherche français ou étrangers, des laboratoires publics ou privés.

***Passive Online RTT Estimation  
for Flow-Aware Routers using One-Way Traffic***

Damiano Carra — Konstantin Avrachenkov — Sara Alouf — Alberto Blanc — Philippe  
Nain — Georg Post

**N° 7124 — version 3**

initial version 26 November 2009 — revised version 3 Decembre 2009

---

 ***apport  
de recherche***

---



## Passive Online RTT Estimation for Flow-Aware Routers using One-Way Traffic

Damiano Carra<sup>\*</sup>, Konstantin Avrachenkov<sup>†</sup>, Sara Alouf<sup>†</sup>, Alberto  
Blanc<sup>†</sup>, Philippe Nain<sup>†</sup>, Georg Post<sup>‡</sup>

Thème : Networks and telecoms  
Équipe-Projet Maestro

Rapport de recherche n° 7124 — version 3<sup>§</sup> — initial version 26 November  
2009 — revised version 3 Decembre 2009 — 22 pages

**Abstract:** With the introduction of the new generation of high speed routers, and with the help of “flow-aware” traffic management, it becomes possible to improve the Quality of Service, the Quality of Experience for users and the network efficiency for ISPs. An example of the “flow-aware” traffic management is the Alcatel-Lucent “Semantic Networking” framework where short-lived and long-lived TCP flows are treated differently. Short-lived flows are processed with high priority and long-lived flows are controlled on a per flow basis. In order to control efficiently the long-lived flows, it is useful to know an estimate of the Round Trip Time (RTT). In the present work, we provide an online RTT estimation algorithm which is passive and needs one-way traffic only. The one-way traffic requirement is essential for the application of the algorithm for “flow-aware” traffic management inside the network. To the best of our knowledge, there was no online one-way traffic RTT estimators. Tests on the Internet demonstrate high accuracy of the proposed estimator. The results show that, 75% (resp. 99%) of the time, the RTT estimate is within 10% (resp. 20%) of the RTT at the source.

**Key-words:** RTT estimation, flow-aware networking, Lomb-Scargle periodogram

<sup>\*</sup> University of Verona, Verona, Italy, damiano.carra@univr.it

<sup>†</sup> Maestro group, INRIA, Sophia Antipolis, France, {firstname.lastname}@sophia.inria.fr

<sup>‡</sup> Alcatel-Lucent Bell Labs, Nozay, France, georg.post@alcatel-lucent.fr

<sup>§</sup> This third version includes a new figure in Section 5.1, that is Fig. 5.

**Résumé :** Grâce au déploiement de la nouvelle génération de routeurs à grande vitesse, il est dorénavant possible d'améliorer la Qualité de Service perçue par les utilisateurs et l'efficacité du réseau en adoptant un ordonnancement par flot. Un exemple de cette approche est le concept de "Semantic Networking" développé en collaboration avec Alcatel-Lucent. Il s'agit ici de différencier le traitement des flots selon leur durée. Ainsi, les flots courts sont prioritaires alors que les flots de longue durée sont contrôlés au cas par cas. Pour être efficace, le contrôle d'un flot TCP de longue durée nécessite une estimation du délai aller-retour (*Round Trip Time* ou RTT).

Dans ce rapport, nous développons un algorithme pour l'estimation du RTT qui peut être exécuté dans un routeur au cœur du réseau. Cet algorithme n'injecte pas de paquets dans le réseau et utilise uniquement le trafic observé dans le sens source-destination. De plus, il s'exécute en ligne produisant une nouvelle estimation du RTT à chaque paquet du flot considéré. L'algorithme a été validé sur une plate-forme expérimentale et sur Internet. Les expérimentations menées montrent que l'algorithme prédit la valeur du RTT avec une grande précision.

**Mots-clés :** estimation du RTT, ordonnancement par flot, périodogramme de Lomb-Scargle

## Contents

|          |   |           |
|----------|---|-----------|
| <b>1</b> | <b>Introduction</b>                             | <b>3</b>  |
| <b>2</b> | <b>Related Work</b>                             | <b>5</b>  |
| <b>3</b> | <b>Motivations</b>                              | <b>6</b>  |
| 3.1      | Flow-Aware Networking . . . . .                 | 6         |
| 3.2      | Novel AQM Policies . . . . .                    | 7         |
| <b>4</b> | <b>A methodology Based on Spectral Analysis</b> | <b>9</b>  |
| <b>5</b> | <b>Estimation Process</b>                       | <b>10</b> |
| 5.1      | Online Lomb Periodogram . . . . .               | 11        |
| 5.2      | Fundamental Frequency Extraction . . . . .      | 12        |
| <b>6</b> | <b>On the Estimation Accuracy</b>               | <b>14</b> |
| <b>7</b> | <b>Numerical Results</b>                        | <b>15</b> |
| 7.1      | Controlled Environment . . . . .                | 16        |
| 7.2      | Internet Experiments . . . . .                  | 19        |
| <b>8</b> | <b>Open Issues and Conclusions</b>              | <b>20</b> |

## 1 Introduction

Customers' increasing demand for better quality of service (QoS) and quality of experience (QoE) [5] have increased the interest in techniques for actively managing and controlling the traffic inside the network. With the introduction of the new generation of high speed routers, it becomes possible to treat individually a significant number of flows. An example of "flow-aware" traffic management is Alcatel-Lucent's framework of "Semantic Networking;" a detailed description can be found in [10].

The framework "Semantic Networking" takes advantage of the *mice-elephants* phenomenon. Many measurement studies have observed that the traffic is approximately composed of two types of connections: short-lived and long-lived flows, also known as *mice* and *elephants*. It has been observed that the number of flows of each type and the actual traffic they generate can be summarized by the 80-20 rule: mice account for the majority of the flows (80%), but the volume of the traffic associated to them represents 20% of the total traffic, while elephants (20% of the flows) convey 80% of the total traffic. Recent measurements [5] show that this proportion is shifting to a 90-10 rule. Therefore, by serving the short-lived flows with high priority one can significantly decrease the number of active flows. The efficiency of such approach has been validated by [2, 12]. For the long-lived flows, it has been observed that the instantaneous number of elephants present in the router is small, actually only few hundreds [8]. This means that it is possible to manage long-lived flows on per flow basis. Such an approach can give to an ISP a greater flexibility in managing its network, potentially increasing its performance and its efficiency and providing customers with high QoS and QoE [10].

One of the most important notions for a TCP flow is its aggressiveness that is how fast a TCP connection increases its sending rate. Most deployed TCP versions are based on a congestion window which limits the number of packets that can be sent during one Round Trip Time (RTT) and use a congestion control algorithm that acts every RTT. This implies that the RTT is one of the principal parameters which determine the aggressiveness of a TCP flow, and it needs to be taken into account for the design of new “flow-aware” traffic management schemes.

In this report, we present an algorithm for the *online* estimation of the RTT by passively monitoring, in real-time, only one direction of a TCP flow. Specifically, our algorithm satisfies different constraints. The estimation is passive, as the measuring point (e.g., the router) does not inject packets into an existing flow, nor does it alter their flow. The estimation is done in *real-time*, since the flow rate and its rate growth should be instantaneously available at the measuring point. This constraint implies that the used algorithms must be both computationally efficient and working incrementally as new packets arrive. In other words, we need to find efficient *online* algorithms that provide sufficiently accurate results. The last constraint imposes the use of information on only *one direction* of a TCP flow. One cannot assume that the monitoring point sees packets in both directions as forward and reverse paths may be different. Furthermore, even when forward and reverse traffic do flow through the monitoring point, collecting and real-time processing of two-way traffic may impose excessive load and complexity on the network cards.

As we will discuss in detail in the ensuing section on related work, none of the existing methods for RTT estimation satisfies simultaneously the above mentioned criteria.

Our work makes the following important contributions. We design a method for RTT estimation based on the traffic observed only in one direction. The method relies on spectral analysis of the signal built considering the inter-packet times. The self-clocking mechanism of TCP introduces *periodic* components into the arrival times of packets. We use spectral analysis to extract such periodic components. There are different tools available for spectrum estimation, mainly for regularly sampled data. The samples collected at the router are irregularly spaced, thus the choice is essentially limited, for either technical or computational reasons, to the *Lomb periodogram*. The typical implementation of any spectral analysis tool uses an offline approach. Our main contribution is the development of an online version of the Lomb periodogram. At each packet arrival, the estimation of the spectrum is updated with  $O(N)$  operations, where  $N$  is the length of the initial sequence collected (the number of frequencies in the spectrum is  $2N$ ).

Another contribution lies in the fundamental frequency extraction algorithm: once the estimation of the spectrum is done, we need to extract the fundamental frequency that corresponds to the inverse of the RTT. This is done using a pattern matching technique that looks for the greatest common divisor of a subset of frequencies.

We tested our estimation algorithm both on a controlled testbed and on the Internet. The results show that our solution is able to accurately estimate the RTT, the estimation error being within  $\pm 10\%$  (resp.  $\pm 20\%$ ) of the true value with probability equal to 75% (resp. 99%). The results given by our methodology show a higher accuracy with respect to the results obtained in previous

studies (see Section 2 for a review of the literature), using less information, namely packets flowing in only one direction.

The remainder of this report is organized as follows. In Sections 2 and 3, we present in detail our motivations and related works. In Section 4, we discuss the application of spectral analysis. In Section 5, we present our methodology for the estimation of the RTT, describing the building blocks that compose the solution. In Section 6, we highlight the issues related to the accuracy of the estimation. In Section 7, we report the results of the evaluation of our methodology. Finally, in Section 8, we present our conclusions and discuss some possible extensions.

## 2 Related Work

The RTT estimation has been the subject of many studies. The aim of these studies is to understand the characteristics of the TCP connections in the Internet, in order to study different aspects, such as the rate-limiting factors or the non-conforming TCP senders. These works consider methods that can be applied offline, since they are generally computationally intensive. For instance, the work of S. Jaiswal et al. in [6] is based on the reconstruction of the TCP congestion window values, which requires to maintain a “replica” of the TCP sender’s state. This work was later extended by J. But et al. in [4], maintaining however the computational complexity.

Another example is the work of Y. Zhang et al. who propose in [17] a method based on time correlation of samples: while the computational complexity is similar to our approach, the main problem is related to robustness, since the results are strongly affected by noise, which impacts the accuracy of the RTT estimation.

In [9], R. Lance et al. make use of spectral analysis—the basic mechanism used by our solution—as one of the possible steps for off-line estimation of the RTT. In particular, the authors apply the spectral analysis to a set of samples, but they do not consider the continuous, real-time update of the spectrum as new samples arrive. Moreover, the post processing of the spectrum for the extraction of the RTT is based on a simple evaluation of the frequency with the maximum power, which not always corresponds to the fundamental frequency.

In [16], B. Veal et al. propose a method based on the TCP timestamp option. Our method does not rely on information provided by the protocols, but it is based only on the inter-arrival times of the packets. In [7], Jiang and Dovrolis estimate the RTT using the first packets of a connection, this method is therefore not generally applicable to the continuous monitoring of a connection.

In [11], Y. Qi et al. propose a method for Bayesian spectrum estimation based on Kalman filtering. Nevertheless, this method is not applied to RTT estimation. The main issue is its complexity: the filter gain computation requires a matrix multiplication, whose complexity is approximately  $O(N^{2.8})$  ( $N$  is the number of samples used); there exist algorithms with  $O(N^{2.376})$ , but with much higher constants, which makes them practically unusable. Our methodology has a complexity of  $O(N)$  at each sample arrival, since  $2N$  is the number of frequencies in the spectrum (see Section 5), thus, if we consider  $N$  consecutive samples, the complexity becomes  $O(N^2)$ .



In summary, all the previous works have some limitations that make them not applicable to the context we are considering: Since we are looking for real-time (online) estimation of the RTT inside a router (see Section 3 for details), the proposed methods cannot be used for their computational complexity or the low accuracy. Note also that some methodologies (works in [6, 4, 16]) use traffic captured in both directions, and correlate packets with their acknowledgments. Our methodology uses packets of only one direction (thus we use less information) yet obtaining a more accurate estimation of the RTT.

### 3 Motivations

The methods proposed so far for estimating the RTT have focused on the evaluation of the characteristics of the TCP connections for monitoring purposes: the interior monitoring point collects packets from a router interface (e.g. from both directions of a network card) and the traces are analyzed offline. In this report, we have a completely different point of view. The estimation of the RTT is a building block for actively controlling the traffic inside the network. We start considering a flow-aware networking approach, where routers are able to manage flows rather than simply packets. This in turn opens the possibility of exploring novel Active Queue Management (AQM) techniques in order to efficiently manage the router resources.

#### 3.1 Flow-Aware Networking

Customers' increasing demand for better quality of service (QoS) and quality of experience (QoE) have increased the interest in techniques for actively managing and controlling the traffic inside the network. One such approach calls for treating each flow individually, where by flow we mean a connection identified by the classical five-tuple of protocol ID, source and destination addresses and ports. Considering a flow as the basic entity to deal with, rather than single packets, has a beneficial impact on scalability, flexibility and operational complexity. For a detailed view of the flow-aware networking approach the interested reader is referred to [10]. Here we consider the practical implementation of such an approach, and in particular the structure of a *flow-aware* router.

The basic architecture considered is depicted in Fig. 1. There is a single physical buffer that is divided into a number of virtual queues, one of which has high priority and the others have low priority. Flows are sorted into two classes, whether they are short-lived or long-lived flows. The basic idea is to put all the short-lived flows in the high priority queue, and to assign a low priority queue to each of the long-lived flows. When a new flow arrives, it is initially treated as short-lived. If the cumulative number of packets of a given flow reaches a threshold, this flow is then considered as an elephant, i.e., its packets are enqueued in a low priority queue associated to this flow.<sup>1</sup> Low priority queues are served in a round robin fashion or a similar scheduling policy.

<sup>1</sup>There exist a number of different mechanisms to “promote” a flow to elephant, mainly probabilistic methods. For instance, each arriving packet is compared with one or more packets randomly picked from the buffer: if the packets belong to the same flow, then this flow can be considered with high probability an elephant.

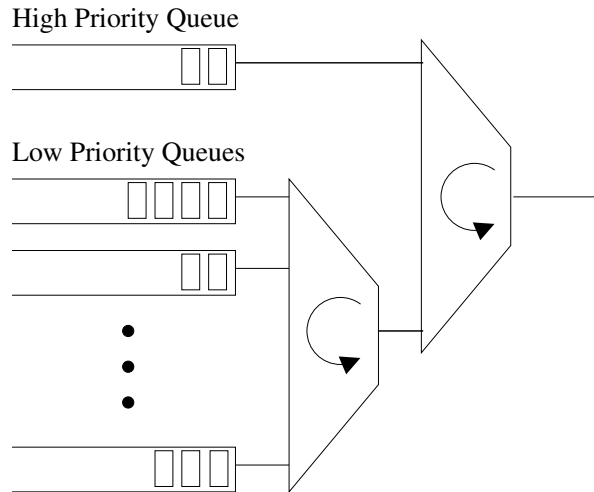


Figure 1: Buffer management: basic scheme of a flow-aware router. Short-lives flows (90% of the flows, 10% of the total traffic) are stored in a single high-priority queue, while each long-lived flow has a low-priority queue. Low priority queues are served in a round-robin fashion.

It has been observed in [8] that the number of concurrent long-lived flows at a router is of the order of hundreds. This means that it is possible, with the current technology, to individually manage these flows. Moreover, since they carry 90% of the total traffic, by controlling elephants, it is possible to manage accurately the available resources.

### 3.2 Novel AQM Policies

Flows for large data transfers use TCP to compete for bandwidth. More specifically, they use window based congestion control, where each flow increases its sending rate until a packet loss is detected (or an explicit congestion notification is received). Conventional routers that are not flow-aware cannot insure fairness under high traffic loads, especially when the competing flows have different RTTs [3, 1].

With flow-aware routers, there is the possibility of new flow-aware queue management algorithms capable of proactively controlling each flow. Being able to predict the behavior of a flow can be very useful in order to achieve this goal. In the case of a TCP connection, its future behavior (in the absence of a packet drop or congestion signal) is dictated by the increase of the congestion window. The rate of the increase depends on the RTT, as the congestion window is incremented by one or more packets each RTT. Therefore, tracking in real time this parameter is a fundamental step in predicting the evolution of a flow. While the RTT is available at the sender, current TCP versions do not propagate this information to the routers; only experimental protocols like XCP convey this information explicitly.

Furthermore, if the RTT is known, it is possible to better estimate the flow rates: by averaging the number of packets received within an interval equal to RTT it is possible to correctly estimate the TCP throughput; cf. Fig. 2. A

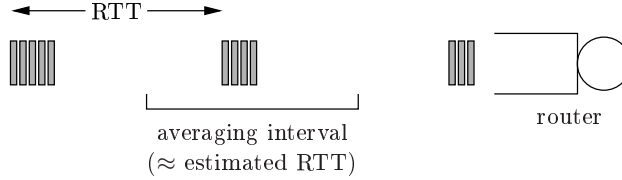


Figure 2: Rate estimation using the RTT: a fair estimation of the RTT allows for a stable estimation of the rate.

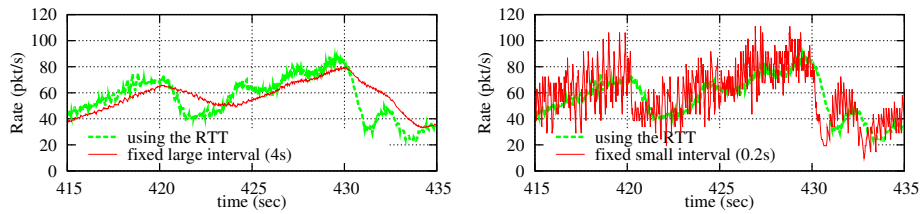


Figure 3: Rate estimate using the estimated RTT, compared with the same using two fixed averaging intervals: large interval (left) and small interval (right).

smaller value of the averaging interval results in a fluctuation of the estimate, while a bigger value does not allow for a prompt detection of rate changes (e.g., due to dropped packets). This is illustrated in Fig. 3, which shows an experiment's rate estimation made with our estimation tool (cf. Section 5), compared with the same using fixed averaging intervals; the experiment is `expl`; cf. Section 7.

If the information about the rate and its growth is made available at the router, it is then possible to design novel AQM policies that take into account this information. For instance, consider the scenario with two competing flows that are saturating the available bandwidth, i.e., the buffer occupation starts increasing. Assume that both flows have, at a given point in time, the same instantaneous rate, but different RTTs (which means the instantaneous flow rates have different *growth* rates). The router may decide to mark/drop in advance packets belonging to one or both flows, before the buffer becomes full. By knowing the RTT, it is possible to choose, for instance, the more aggressive flow, i.e., the flow with the smaller RTT.

While the study of novel AQM policies is not the focus of this report, we highlight that the estimation of the RTT represents an important building block for such policies. Note that previously proposed schemes (e.g. [6, 4]) cannot be used in such a context, since they assume to have access to the traffic in both directions. Such solutions would be technologically and computationally infeasible inside a router, since they require the router itself not only to correlate packets with their acknowledgments, but also to do so in real-time, in order to make the information available, in real-time, for correctly applying the AQM policy.

In summary, while the RTT estimation is a well covered area of research, no techniques are available for the continuous, real-time and passive estimation of the RTT, using the traffic of one direction.

## 4 A methodology Based on Spectral Analysis

The self-clocking mechanism of TCP introduces *periodic* components into the arrival times of packets, the main one being the RTT. The basic idea of the RTT estimation is to use spectral analysis to extract such periodic components. With spectral analysis, it is possible to build an estimation of the spectrum of a signal starting from a finite sequence of samples. There is a large set of useful methods suitable for different scenarios [14]. In order to choose the best method, the first step in spectral analysis is to identify the characteristics of the *signal* whose spectrum is to be estimated.

In our case, the signal is the packet inter-arrival time of the flow at hand. This signal is sampled at each packet arrival. More precisely, at the arrival of the  $k$ th packet of the flow at hand, a new sample of the signal is computed, namely  $h_k := t_k - t_{k-1}$ , with  $k \geq 1$  where  $t_k$  is the arrival instant of the  $k$ th packet and  $t_0 := 0$ . Since samples are taken at packet arrivals, the sequence  $h_k$  is unevenly spaced. The signal is said to be *irregularly* sampled (also unevenly sampled or nonuniformly sampled). While the literature on regularly sampled data proposes many efficient methods to estimate the signal's spectrum, the proposed solutions for irregularly sampled data have been found to be impractical [15]: The choice of spectral analysis for irregularly sampled data is essentially limited, for either technical or computational reasons, to the *periodogram*.

The periodogram is simply the Discrete Fourier Transform (DFT) of the finite sequence. In case of irregularly sampled data, the periodogram is computed using the Lomb-Scargle method [13] and it is generally referred to as the Lomb periodogram. The periodogram has well-known limitations [14]: (i) it is not possible to distinguish two sinusoidal components which are too close (low resolution), and (ii) the variance of the estimation error at a given frequency does not decrease as the number of samples used in the computation increases (non-consistent estimator). Despite these limitations, the periodogram remains an efficient solution in case of well-separated sinusoids in white noise and medium to large dynamic range [15]. The dynamic range is defined as the ratio between the maximum and the minimum power values, usually measured in decibel. A dynamic range between 20 dB and 30 dB (i.e., between two to three orders of magnitude between the maximum and the minimum power) is said to be “medium”; if it is greater than 30 dB, then it is said to be “large.”

In our case, the signal  $h_k$ , the inter-arrival times of the packets, either contains a single strong sinusoidal component, with large dynamic range, due to the RTT, or it does not contain any periodicity (consider the case of a flow that has reached the bandwidth-delay product, where packets form a continuous stream). In the latter case, no method based on spectral analysis is able to extract the RTT: only methods based on the analysis of the traffic in both directions would work—a case that we cannot consider since a flow-aware router has access in real-time only to one direction. Thanks to the characteristics of the signal  $h_k$ , the periodogram does represent a good estimator.

A problem common to all the methods for spectral analysis (for either regularly or irregularly sampled data, including the periodogram) is that they are based on offline algorithms: they consider a sequence of  $N$  samples and they build an estimation of the spectrum. If the signal is composed of more than  $N$  samples, it is divided into subsequences of  $N$  samples and the methodology is applied to each subsequence separately. While this approach can be suitable for

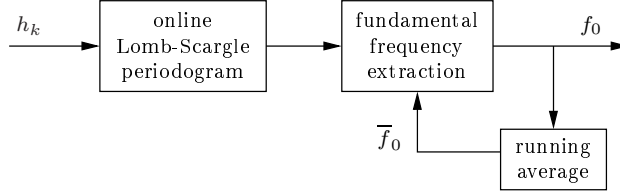


Figure 4: The RTT estimation process: after the update of the spectrum estimation, the fundamental frequency is extracted. The estimation of the RTT is the inverse of the fundamental frequency  $f_0$ .

traditional analysis of signals, it cannot be applied in case of RTT estimation by a flow-aware router. It may take several RTTs before being able to collect  $N$  samples (typical values of  $N$  are 256, 512 or 1024). If the RTT varies, the router is not able to correctly follow these variations, leading to a wrong estimation of the flow rates, with negative consequences on the efficiency of the AQM policies.

It is extremely important to have a spectrum estimation methodology that works in real time, i.e., that is able to update the estimate at each packet arrival. The solution should also be computationally efficient. The simplicity of the periodogram helps in designing an *online* version of the method. All the other methods (even the more advanced ones recently proposed for irregular sampled data, see [15]) are based on complex optimized algorithms, and cannot be translated into corresponding online versions.

In summary, among the different methods for spectral analysis, the periodogram represents the only choice for two reasons:

- the structure of the signal  $h_k$  (with a single strong sinusoidal component) makes the periodogram a sufficiently good estimator, overcoming its limitations;
- the periodogram allows for the creation of an efficient online version of the algorithm, something not possible in the case of irregularly sampled data with other proposed spectral analysis approaches.

The spectral analysis represents the basic building block of our RTT estimation method: the whole estimation process is composed of different steps that we describe in detail in the following section.

## 5 Estimation Process

At each packet arrival a new sample is added to the sequence  $h_k$ . The estimation process takes as input the new packet arrival time and updates the current estimation of the RTT. Figure 4 shows the functional blocks of the estimation process.

Given a periodic discrete signal, with period  $T_0$  and frequency  $f_0 = 1/T_0$ , the periodogram of the signal presents peaks at frequencies  $f_0, 2f_0, 3f_0, \dots$ , where  $f_0$  is called the *fundamental frequency*. In general, the highest peak in the periodogram is not necessarily at  $f_0$ , but it can be at any multiple of  $f_0$ ; therefore, it is not sufficient to look for the largest peak in the spectrum to find  $f_0$ . For this reason, we need another module to extract the fundamental frequency.

This module takes as input a list of the spectrum peaks and the average of the previous estimations. The fundamental frequency is extracted with a pattern-matching technique. Basically, after smoothing the periodogram through a low-pass filter, we take the largest  $W$  peaks and iteratively search for the frequency in the list that is the least common divisor of the other frequencies in the list.

### 5.1 Online Lomb Periodogram

The Lomb-Scargle periodogram [13] is built using  $N$  samples. Once the initial  $N$  samples are collected and the Lomb periodogram is built, every time a new packet arrives, the oldest sample is removed and the new sample is used to update the Lomb periodogram.

The offline version of the Lomb periodogram takes  $O(N \log N)$  operations. To the best of our knowledge, no online implementation (i.e., update of the periodogram as the samples arrive) exists, so we had to devise one. For the online computation, we start from the definition of the Lomb periodogram. The power spectrum (Lomb periodogram), at angular frequency  $\omega := 2\pi f$ , and at the  $k$ th sample with  $k \geq N$ , is

$$P_k^N(\omega) := \frac{1}{2\sigma_k^2} \left\{ \frac{\left[ \sum_{j=0}^{N-1} (h_{k-j} - \bar{h}_k) \cos \omega(t_{k-j} - \tau_k) \right]^2}{\sum_{j=0}^{N-1} \cos^2 \omega(t_{k-j} - \tau_k)} + \frac{\left[ \sum_{j=0}^{N-1} (h_{k-j} - \bar{h}_k) \sin \omega(t_{k-j} - \tau_k) \right]^2}{\sum_{j=0}^{N-1} \sin^2 \omega(t_{k-j} - \tau_k)} \right\} \quad (1)$$

where  $\bar{h}_k$  and  $\sigma_k^2$  are the mean and variance of the  $N$  last samples of the sequence  $h_k$ :

$$\bar{h}_k := \frac{1}{N} \sum_{i=0}^{N-1} h_{k-i} = \bar{h}_{k-1} + \frac{h_k - h_{k-N}}{N}; \quad (2)$$

$$\begin{aligned} \sigma_k^2 &:= \frac{1}{N-1} \sum_{i=0}^{N-1} h_{k-i}^2 - \frac{N}{N-1} \bar{h}_k^2 \\ &= \sigma_{k-1}^2 + \frac{h_k^2 - h_{k-N}^2}{N-1} + \frac{N}{N-1} (\bar{h}_{k-1}^2 - \bar{h}_k^2), \end{aligned} \quad (3)$$

and where  $\tau_k$  is the solution of

$$\tan(2\omega\tau_k) = \frac{\sum_{i=0}^{N-1} \sin 2\omega t_{k-i}}{\sum_{i=0}^{N-1} \cos 2\omega t_{k-i}}. \quad (4)$$

The summations in (2) and (3) can be efficiently updated at each packet arrival.

The periodogram (1) is evaluated for a number of frequencies equal to  $2N$ . In particular, we compute the minimum frequency at arrival of packet  $k$ ,  $f_k^{\min}$ , considering the interval of time of the  $N$  current samples, i.e.,  $f_k^{\min} = 1/(t_k - t_{k-N+1})$ . The maximum frequency,  $f_k^{\max}$ , is derived from the Nyquist theorem: since we have  $N$  samples, we obtain  $f_k^{\max} = \frac{N}{2} f_k^{\min}$ . The interval  $[f_k^{\min}, f_k^{\max}]$  is divided into  $2N$  values, obtaining  $\Delta_\omega = 2\pi \frac{f_k^{\max} - f_k^{\min}}{2N}$ . Thus, we compute  $P_k^N(\omega_i)$  for every  $\omega_i = 2\pi f_k^{\min} + i\Delta_\omega$ ,  $i = 0, \dots, 2N-1$ .

The power spectrum is to be updated at each packet arrival. Since the values of  $\tau_k$  and  $\bar{h}_k$  change at each packet arrival, the summations in (1) must be always recomputed. This can be avoided by decomposing (1) using basic trigonometric properties. We define

$$\begin{aligned}\Phi_k &:= \sum_{j=0}^{N-1} h_{k-j} \cos(\omega t_{k-j}) - \bar{h}_k \sum_{j=0}^{N-1} \cos(\omega t_{k-j}); \\ \Gamma_k &:= \sum_{j=0}^{N-1} h_{k-j} \sin(\omega t_{k-j}) - \bar{h}_k \sum_{j=0}^{N-1} \sin(\omega t_{k-j}); \\ \Phi_k^* &:= \sum_{j=0}^{N-1} \cos(2\omega t_{k-j}); \\ \Gamma_k^* &:= \sum_{j=0}^{N-1} \sin(2\omega t_{k-j}).\end{aligned}$$

Note that  $\Phi_k$ ,  $\Gamma_k$ ,  $\Phi_k^*$  and  $\Gamma_k^*$  are simple summations that can be updated at each packet arrival in a similar way as done for (2)-(3). We can then rewrite the Lomb periodogram as follows:

$$\begin{aligned}P_k^N(\omega) &= \frac{1}{\sigma_k^2} \left\{ \frac{[\Phi_k \cos(\omega \tau_k) + \Gamma_k \sin(\omega \tau_k)]^2}{N + \Phi_k^* \cos(2\omega \tau_k) + \Gamma_k^* \sin(2\omega \tau_k)} + \right. \\ &\quad \left. + \frac{[\Gamma_k \cos(\omega \tau_k) - \Phi_k \sin(\omega \tau_k)]^2}{N - \Phi_k^* \cos(2\omega \tau_k) - \Gamma_k^* \sin(2\omega \tau_k)} \right\}. \quad (5)\end{aligned}$$

When a new packet  $k$  arrives, the values of  $\bar{h}_k$ ,  $\tau_k$ ,  $\sigma_k^2$ ,  $\Phi_k$ ,  $\Gamma_k$ ,  $\Phi_k^*$  and  $\Gamma_k^*$  are immediately updated, and the Lomb periodogram is recomputed accordingly. The number of operations necessary at each packet arrival is  $O(N)$ , since updating  $\bar{h}_k$ ,  $\tau_k$ ,  $\sigma_k^2$ ,  $\Phi_k$ ,  $\Gamma_k$ ,  $\Phi_k^*$  and  $\Gamma_k^*$  takes  $O(1)$  and we have  $2N$  angular frequencies  $\omega$ .

For illustration purposes, we depict in Fig. 5 the periodogram computed using (5) on a Caida trace. Each graph corresponds to a single snapshot where the fundamental frequency is indicated with a double cross.

## 5.2 Fundamental Frequency Extraction

The outcome of the computation of the Lomb periodogram is usually *noisy*, with many local maxima and a global maximum that not always corresponds to the fundamental frequency  $f_0$ : sometimes the global maximum corresponds to a frequency multiple of the fundamental one (see for instance Fig. 5). The

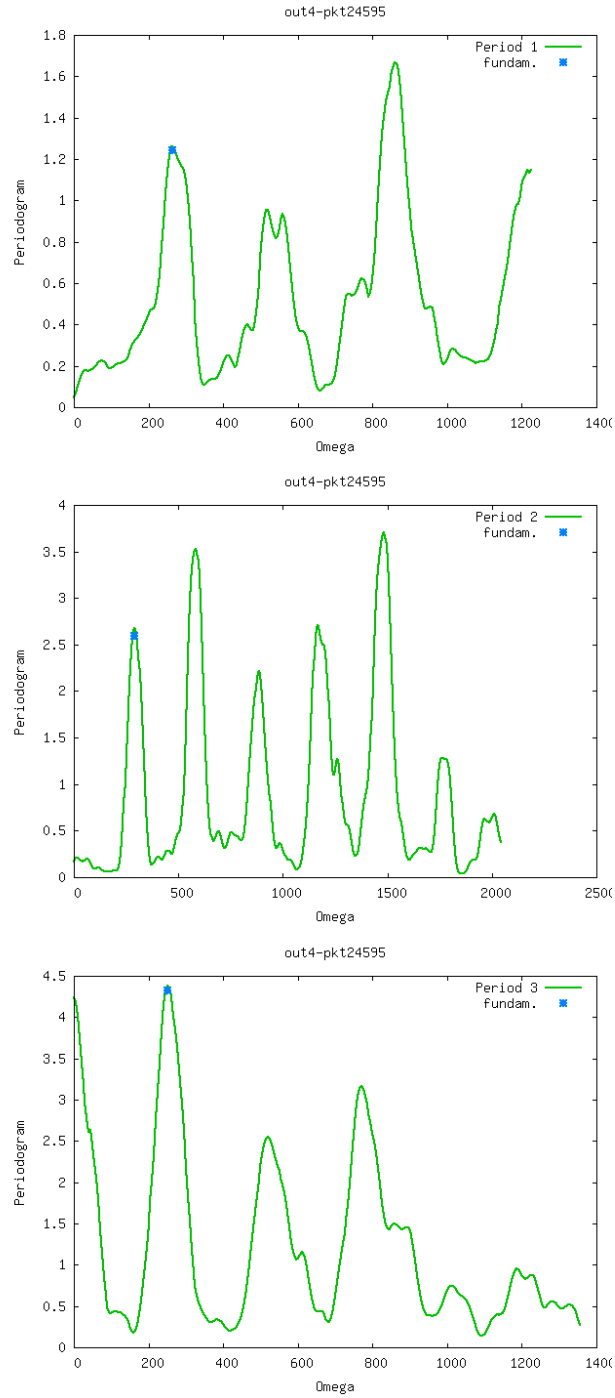


Figure 5: Periodogram of Caida trace out4-pkt24595 at three points in time.

operations performed *at each packet arrival* by the Fundamental Frequency Extraction module on the updated periodogram can be summarized as follows:



**Periodogram smoothing.** A basic low-pass FIR filter is applied to the sequence that composes the Lomb Periodogram: in particular, the filter is a moving average filter of order three. We have tested different orders for the filter obtaining similar results, as long as the order is not too high (e.g., greater than 8), since the smoothing effect decreases the dynamic range.

**Peak detection.** We consider the value at frequency  $f_k$  to be a peak if it is greater than the values at frequencies  $f_{k+1}$  and  $f_{k-1}$ ; the detected peaks are put in a “peak list.”

**Peak pruning and ordering.** We remove from the list the entries whose values are not the top  $W$  largest peaks, with  $W = 10$ . The parameter  $W$  is configurable: in all our experiments, the number of peaks in the spectrum was between 15 and 25, but only a subset of them were sufficiently strong (one order of magnitude greater than the white noise). By considering the average characteristics of the TCP flows observed in [6], we can conclude that this value can be applied in general. From the peak list, we remove also some frequency values considering the following boundary conditions: the RTT should be greater than 2 ms and less than 500 ms. In [6], it has been observed that 70% of the flows have RTT smaller than 500 ms. The list is then ordered by frequency, smallest first.

**Multiple frequency search.** Starting from the smallest frequency in the list, we evaluate if the other frequencies in the list can be a multiple of the considered frequency. If we find at least two multiples, this step ends and returns the estimated fundamental frequency  $f_0$ . Otherwise it goes on with the following value in the list. If no fundamental frequency is found, this step returns a *NULL* value.

**Comparison.** We compare the output with the average of the previous estimations,  $\bar{f}_0$ . If the current estimation is not *NULL*, we consider the ratio between the current estimation and the average of the previous estimations,  $r = f_0/\bar{f}_0$ . In [6], the authors show that, in 95% of the flows, the ratio between the maximum and the minimum RTT is less than  $3/2$ . Thus, if  $2/3 < r < 3/2$ , the algorithm returns  $f_0$  and terminates. Otherwise, it returns  $\bar{f}_0$ .

The output of this module is then the estimated fundamental frequency whose inverse is the estimated RTT.

## 6 On the Estimation Accuracy

In this section, we consider the problem of *what* actually we are measuring when we apply our methodology. Due to many factors, the instantaneous RTT (at the source) may be highly variable: part of the RTT, in fact, is due to the queueing delay inside routers. When queues start growing, the delay increases. When packets of a flow are dropped, the rate is halved (this is the case of many TCP implementations) and the delay suddenly decreases. Since the measuring point is in between the source and the destination of a flow, the estimated RTT will be always different from the real RTT measured at the source. The difference depends mainly on the *variability* of the RTT and the delay between the source and the measuring point. Assume that the different flights of TCP packets are well separated. The RTT measured for the flight  $i$  of packets is  $\text{RTT}_i$ , while the RTT of the flight  $j$  is  $\text{RTT}_j = \text{RTT}_i + \Delta\text{RTT}$ . We define  $\Delta\text{RTT}$  as the

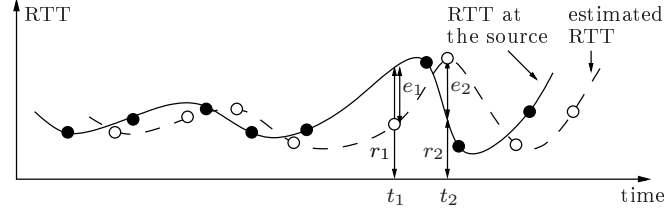


Figure 6: Errors in the RTT estimation process: a highly variable RTT induces bigger instantaneous estimation errors.

variability of the RTT. If  $\Delta\text{RTT}$  is small w.r.t. the RTT (for instance, the mean RTT), then the estimation error would be small. Figure 6 shows an example. Each point in the figure represents a flight of TCP packets. Before  $t_1$ , the variability of the RTT is low and the estimation error is limited, independently from the delay between the source and the measuring point.

If  $\Delta\text{RTT}$  is comparable to the RTT, the estimation error depends strongly on the position of the measuring point. For instance, if the measuring point is close to the source, the estimation should follow closely the variations. If the measuring point is close to the destination (as in the case shown in Fig. 6) the error may be significant.

Since our method uses the traffic of only one direction, it is not possible to know the delay between the source and the measuring point—methods based on the two-way traffic would be able to reconstruct such information. Therefore we are not able to evaluate if the instantaneous error in the estimation is due to the delay or to the accuracy of the spectral analysis. In order to filter out the error due to the delay, we may take the mean values of the RTTs (real and estimated) on a short time frame.

Another problem related to the estimation process is due to the averaging effect of the spectral analysis. Since the spectrum is built using the last  $N$  samples, sudden changes in the RTT may not be detected. In fact the  $N$  samples may contain 5-8 TCP flights. If the variability of the RTT is high, changing for instance every 3-4 flights, then the spectrum will contain samples with different RTTs, and the estimated fundamental frequency may not follow closely the RTT variation. This second contribution to the error cannot be solved by averaging the RTT values. In the following section, we will evaluate to what extent these issues influence the RTT estimation.

## 7 Numerical Results

We validated our methodology with experiments both in a controlled environment and over the Internet. We focus on a single long-lived *scp* transfer between a source and a destination and we collect traces with *tcpdump* at two points: (i) at the source, where we capture the traffic in both directions, in order to have the packets and their acknowledgments; (ii) at a measuring point between the source and the destination, where we record the packets in one direction. In addition to the observed long-lived *scp* transfer, there are different flows on the path between the source and the destination: In the controlled testbed, the cross-traffic flows are generated by *scp* transfers.

The traces collected at the source are post-processed computing the instantaneous RTT and the smoothed RTT using an exponentially weighted moving average (EWMA) algorithm whose parameter  $\alpha$  is set to  $1/8$  (see RFC 2988). Note that the RTT is updated for every packet without considering retransmitted packets.

The traces collected at the measuring point are analyzed using our solution. For the spectral analysis, the length of the sequence considered is  $N = 256$ . The spectral analysis, along with the fundamental frequency extraction, gives the estimation of the instantaneous RTT. Similarly to TCP, we compute a smoothed estimated RTT through an EWMA algorithm with parameter  $\alpha = 1/8$ . Hereinafter, we will use the general term “RTT” to refer to the smoothed value of the RTT (at the source and estimated).

The file size used for the testbed and for the Internet experiments is 120 MBytes. From the samples of the RTTs we create the empirical Cumulative Distribution Function (CDF). From this empirical distribution we can derive any performance index of interest, such as the mean RTT and the variance of the RTT.

In order to evaluate the accuracy of the estimation process over time, we consider the error between the estimation and the real RTT. To overcome the issues highlighted in Section 6, we consider the means of the RTTs (estimated and at the source) taken over small, non overlapping, intervals. In practice, we compute the mean RTTs every 5 seconds and we compute the error of the estimate defined as

$$\text{error} = \frac{\text{mean estimated RTT} - \text{mean RTT at the source}}{\text{mean RTT at the source}}.$$

From the error, we build the corresponding empirical CDF.

## 7.1 Controlled Environment

We first considered a testbed set up at INRIA using Dell Precision 380 workstations running Fedora Linux version 10 (kernel 2.6.27). The topology is shown in Fig. 7: all machines are directly connected as shown (using Ethernet cables) and there is no outside traffic. Given that the propagation and processing delay are very small, we introduce random delays between the machines. The link between the source of the traffic and the machine *cross* has a delay uniformly distributed on  $[50 - d_1, 50 + d_1]$  ms, where  $d_1$  is set to either 5 or 40 ms. The link between the machines *cross* and *btlnk* has a delay uniformly distributed on  $[25 - d_2, 25 + d_2]$  ms, where  $d_2$  is set to either 5 or 20 ms.

All the links have a capacity of 100 Mbps (fast Ethernet) except the link between the machines *btlnk* and *dest* which is capped to 10 Mbps in order to act as the bottleneck link. The random delays and the capacity limitations are implemented using the Netem kernel module. Throughout the experiments we explicitly configured the sender to use Reno TCP and not Cubic (the default option for kernel 2.6.27).

The main flow we consider is between machines *source* and *dest*. We add additional cross traffic directed to *dest*, starting from *source* and from *cross*. We have a measuring point of the packets’ arrivals at the machine *btlnk*. Table 1 summarizes the experiments done.

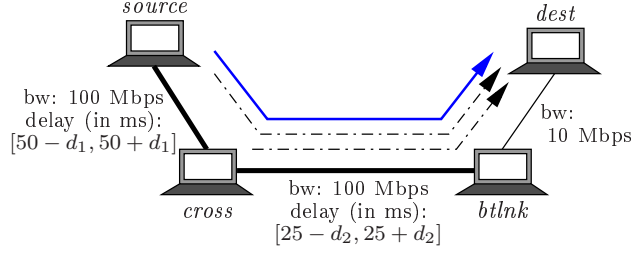


Figure 7: Scheme of the testbed: the continuous line represents the observed flow, dashed lines represent the cross traffic.

Table 1: Configuration of the testbed experiments

| experim.<br>ID | # cross flows<br>$source \rightarrow dest$ | # cross flows<br>$cross \rightarrow dest$ | $d_1$ | $d_2$ |
|----------------|--|---|-------|-------|
| exp1           | 0  | 12  | 5     | 5     |
| exp2           | 2  | 6   | 5     | 5     |
| exp3           | 3  | 9   | 5     | 5     |
| exp4           | 3  | 9   | 40    | 20    |

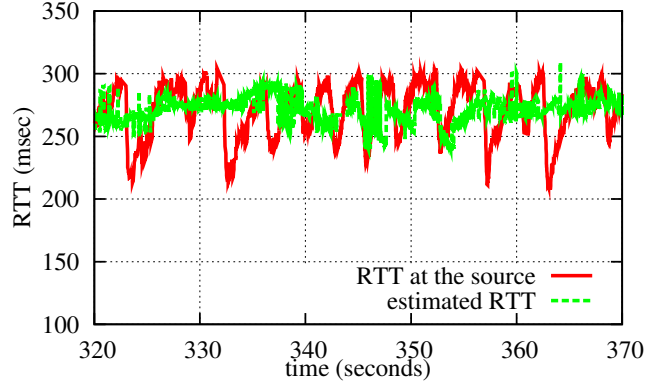


Figure 8: Example of the RTT measured at the source and the estimated RTT (exp2).

Figure 8 shows an example of the output of one experiment (exp2). For each packet, we compute the RTT at the source and its estimation at the measuring point. We have found that the estimated RTT is of the same order of magnitude as the real RTT, even though it seems to be less variable than the RTT at the source. As explained in Section 6, this is due to the averaging effect of the spectral analysis that uses the last observed 256 packets (which include 5-8 flights) for the spectrum estimation.

While this representation shows that the estimation and the real RTT are close, we need to characterize in detail the performance of the algorithm.

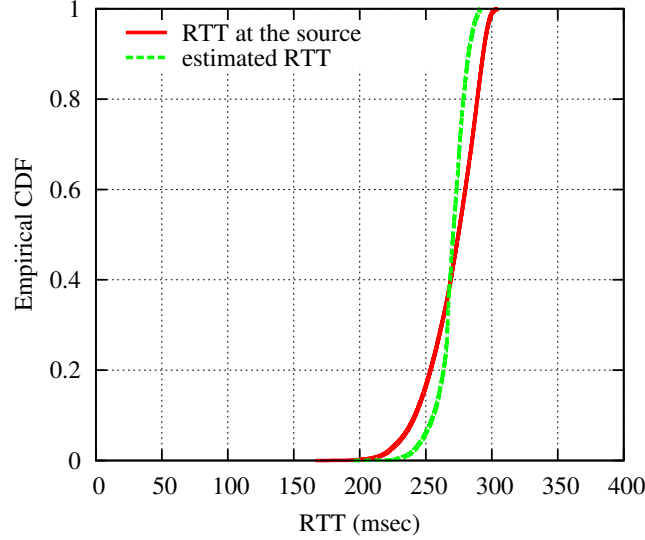


Figure 9: Empirical CDF of the RTT measured at the source and the estimated RTT (exp2).

Table 2: Mean and variance of the RTT (real and estimated): Testbed experiments

| exp.<br>ID | RTT at the source (s) |                        | estimated RTT (s) |                        |
|------------|-----------------------|------------------------|-------------------|------------------------|
|            | mean                  | variance               | mean              | variance               |
| exp1       | 0.2795                | $1.8476 \cdot 10^{-3}$ | 0.2814            | $9.4612 \cdot 10^{-5}$ |
| exp2       | 0.2760                | $1.8431 \cdot 10^{-3}$ | 0.2706            | $1.4061 \cdot 10^{-4}$ |
| exp3       | 0.2782                | $1.6236 \cdot 10^{-3}$ | 0.2792            | $3.5682 \cdot 10^{-6}$ |
| exp4       | 0.2752                | $2.6997 \cdot 10^{-3}$ | 0.2875            | $5.4265 \cdot 10^{-4}$ |

In order to minimize the effects of the lag time between the RTT samples collected at the source and at the measuring point, we consider the empirical cumulative distribution function (CDF) of the RTTs built from the samples. Figure 9 compares the two empirical CDFs (exp2): both CDFs share approximately the same support, i.e., the estimation lies in the same interval of the real RTT.

In Table 2 we report the mean and the variance obtained from the empirical CDFs of the RTTs (real and estimated). While the real RTT has more variability, the estimated RTT is more stable, due to the averaging effect of the spectral analysis.

Another performance index we are interested in is the error in the estimation: as Fig. 10 shows, in experiments exp1–exp3, the estimate lies within 10% of the true value with probability 95%. In the worst case, our solution is able to accurately estimate the RTT with an error in  $[-10\%, 10\%]$  with probability equal to 75%, and with an error in  $[-20\%, 20\%]$  with probability equal to 99%.

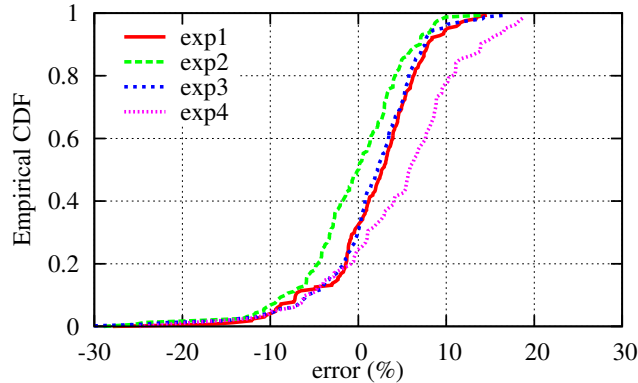


Figure 10: Empirical CDF of the error between the RTT measured at the source and the estimated RTT (testbed).

The results given by our methodology show a higher accuracy with respect to the results obtained in previous studies (e.g. [6]): our results have been obtained observing the traffic in one direction, unlike the results of [6] which require to collect traffic in both directions. In summary, we are able to find an accurate estimation of the RTT using less information w.r.t. previous works, and most noticeably, our method works online.

## 7.2 Internet Experiments

In this section, we show the results of experiments using three machines connected through Internet (Fig. 11). The source is at INRIA Sophia Antipolis (France), the intermediate machine (*hop1*) is at University of Trento (Italy) while the destination is at Eurecom (France). We created two SSH tunnels, one between *source* and *hop1*, and one between *hop1* and the destination *dest*. The traffic generated from the source passes through the tunnel at *hop1*, where packets interarrivals are measured, and reaches the destination. We performed two experiments: the first was done on Sunday 3 May 2009 at 12 PM CEST, whereas the second was done on a week day, namely Monday 4 May 2009, at 10 AM CEST. The *scp* transfer of the 120 MBytes file took 145 seconds in the first experiment and 372 seconds in the second experiment. Hence, we will respectively use the terms “off-peak” and “peak” to refer to these experiments.

Table 3 shows the mean and the variance of the RTTs (real and estimated) for the two “off-peak” and “peak” experiments. It is interesting to observe that the mean RTT is larger during the off-peak hour than during the peak hour. This is most likely due to a change in the routing between the two days the experiments were conducted in.

The high variability of the peak hour results in a higher error, that is not smoothed by considering the overall mean. The reason can be understood looking at Fig. 8: the estimation algorithm often does not detect sudden decreases of the RTT. When the drops in the RTT occur, we obtain large positive error values, while there are not large negative error values to compensate for the large positive ones.

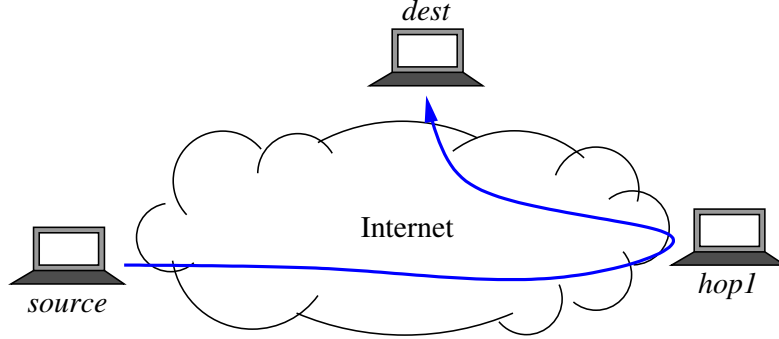


Figure 11: Scheme of the Internet tests.

Table 3: Mean and variance of the RTT (real and estimated): Internet experiments

| exp.<br>ID | RTT at the source (s) |                        | estimated RTT (s) |                        |
|------------|-----------------------|------------------------|-------------------|------------------------|
|            | mean                  | variance               | mean              | variance               |
| peak       | 0.0389                | $1.7194 \cdot 10^{-5}$ | 0.0422            | $2.4034 \cdot 10^{-6}$ |
| off-peak   | 0.0448                | $2.4014 \cdot 10^{-6}$ | 0.0446            | $2.9448 \cdot 10^{-6}$ |

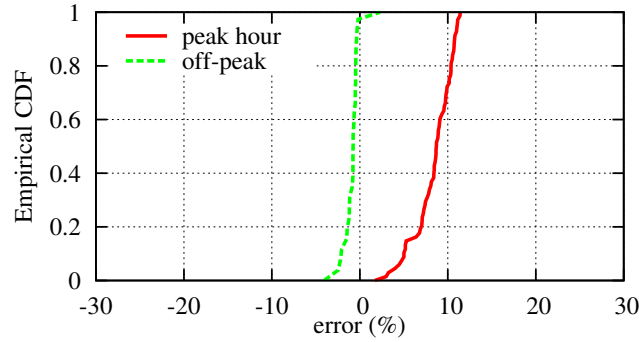


Figure 12: Empirical CDF of the error between the RTT measured at the source and estimated (Internet experiments).

Figure 12 shows the whole empirical CDFs of the error. As for the testbed experiments, the estimate lies within 10% of the true value with probability equal to 99%.

## 8 Open Issues and Conclusions

In this report we have presented a methodology, based on spectrum analysis, for the passive online estimation of the RTT of a long-lived TCP connection, using one-way traffic. The estimation of the RTT represents a basic building

block in the framework of “Semantic Networking,” where flow-aware routers can implement novel AQM techniques in order to control the traffic.

We validate our solution through measurements in a controlled testbed and over the Internet showing a good accuracy. We plan to extend the evaluation using different scenarios: for instance, it is interesting to understand the variation in estimation accuracy as the RTT varies due to changes in the routing or in the number of flows sharing a link.

Since the method is based only on the arrival pattern, it is clear that if the arrival pattern is strongly modified inside the network, the method may not be accurate. For instance, if we observe a flow after it has passed through a bottleneck, the arrival pattern may become a continuous stream of packets. Should this happen, the method may not be applicable, however one would still be able to estimate the rate of a connection through a moving average estimator for instance. In future evaluations, we plan to investigate in detail the scenarios where the methodology may not be accurate, in order to provide a comprehensive view of the benefits of our solution.

## Acknowledgments

This work was done in the framework of the INRIA and Alcatel-Lucent Bell Labs Joint Research Lab on Self Organized Networks.

## References

- [1] E. Altman, T. Jimenez, and R. Nunez Queija. Analysis of two competing TCP/IP connections. *Performance Evaluation*, 49(1-4):43–55, 2002.
- [2] K. Avrachenkov, U. Ayesta, P. Brown, and E. Nyberg. Differentiation between short and long TCP flows: predictability of the response time. In *Proc. of IEEE INFOCOM*, Hong Kong, Mar. 2004.
- [3] P. Brown. Resource sharing of TCP connections with different round trip times. In *Proc. of IEEE INFOCOM*, Tel Aviv, Israel, Mar. 2000.
- [4] J. But, U. Keller, D. Kennedy, and G. Armitage. Passive TCP stream estimation of RTT and jitter parameters. In *Proc. of IEEE 30th Conference on Local Computer Networks*, Sydney, Australia, Nov. 2005.
- [5] D. Collange and J.L. Costeux. Passive estimation of quality of experience. *Journal of Universal Computer Science*, 14(5):625–641, 2008.
- [6] S. Jaiswal, G. Iannaccone, C. Diot, J. Kurose, and D. Towsley. Inferring TCP connection characteristics through passive measurements. In *Proc. of IEEE INFOCOM*, Hong Kong, Mar. 2004.
- [7] H. Jiang and C. Dovrolis. Passive estimation of TCP round-trip times. *Computer Communication Review*, 32(3):75–88, 2002.
- [8] A. Kortebi, L. Muscariello, S. Oueslati, and J. Roberts. Evaluating the number of active flows in a scheduler realizing fair statistical bandwidth sharing. In *Proc. of ACM SIGMETRICS*, Banff, Alberta, Canada, June 2005.



- [9] R. Lance, I. Frommer, B. Hunt, E. Ott, J.A. Yorke, and E. Harder. Round-trip time inference via passive monitoring. *ACM Sigmetrics Performance Evaluation Review*, 33(3):32–38, Dec. 2005.
- [10] L. Noirie, E. Dotaro, G. Carofiglio, A. Dupas, P. Pecci, D. Popa, and G. Post. Self-\* features for semantic networking. In *Proc. of FITraMEN*, Porto, Portugal, Dec. 2008.
- [11] Y. Qi, T.P. Minka, and R.W. Picard. Bayesian spectrum estimation of unevenly sampled nonstationary data. In *Proc. of ICASSP*, Orlando, FL, USA, May 2002.
- [12] I.A. Rai, E.W. Biersack, and G. Urvoy-Keller. Size-based scheduling to improve the performance of short TCP flows. *IEEE Network*, 19(1):12–17, 2005.
- [13] J.D. Scargle. Statistical aspects of spectral analysis of unevenly spaced data. *Journal of Astrophysics*, 263:835–853, 1982.
- [14] P. Stoica and R.L. Moses. *Introduction to spectral analysis*. Prentice-Hall, 1997.
- [15] P. Stoica and N. Sandgren. Spectral analysis of irregularly-sampled data: Paralleling the regularly-sampled data approaches. *Digital Signal Processing*, 16(6):712–734, 2006.
- [16] B. Veal, K. Li, and D. Lowenthal. New methods for passive estimation of TCP round-trip times. In *Proc. of PAM*, Boston, MA, USA, Apr. 2005.
- [17] Y. Zhang, L. Breslau, V. Paxson, and S. Shenker. On the characteristics and origins of Internet flow rates. In *Proc. of ACM SIGCOMM*, Pittsburgh, PA, USA, Aug. 2002.



---

Centre de recherche INRIA Sophia Antipolis – Méditerranée  
2004, route des Lucioles - BP 93 - 06902 Sophia Antipolis Cedex (France)

Centre de recherche INRIA Bordeaux – Sud Ouest : Domaine Universitaire - 351, cours de la Libération - 33405 Talence Cedex  
Centre de recherche INRIA Grenoble – Rhône-Alpes : 655, avenue de l'Europe - 38334 Montbonnot Saint-Ismier  
Centre de recherche INRIA Lille – Nord Europe : Parc Scientifique de la Haute Borne - 40, avenue Halley - 59650 Villeneuve d'Ascq  
Centre de recherche INRIA Nancy – Grand Est : LORIA, Technopôle de Nancy-Brabois - Campus scientifique  
615, rue du Jardin Botanique - BP 101 - 54602 Villers-lès-Nancy Cedex  
Centre de recherche INRIA Paris – Rocquencourt : Domaine de Voluceau - Rocquencourt - BP 105 - 78153 Le Chesnay Cedex  
Centre de recherche INRIA Rennes – Bretagne Atlantique : IRISA, Campus universitaire de Beaulieu - 35042 Rennes Cedex  
Centre de recherche INRIA Saclay – Île-de-France : Parc Orsay Université - ZAC des Vignes : 4, rue Jacques Monod - 91893 Orsay Cedex

---

Éditeur  
INRIA - Domaine de Voluceau - Rocquencourt, BP 105 - 78153 Le Chesnay Cedex (France)  
<http://www.inria.fr>  
ISSN 0249-6399